Pre- filtering of turbulent vector fields in the geodynamo

Patrick Rüdiger* Christopher Weber† Hiroaki Matsui‡ Eric Heien‡ Louise H. Kellogg‡
Bernd Hamann† Hans Hagen*

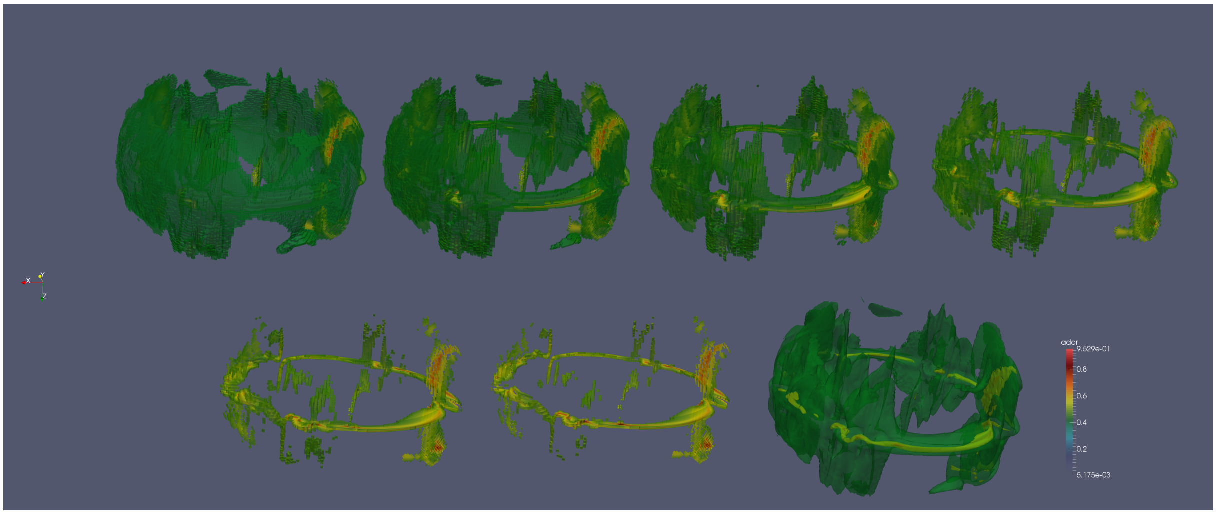

Figure 1: Image sequence showing emergence of turbulent magnetic field behavior. The highly turbulent region showing as a "ring" aligned with the Earth's equator is emphasized in these volume visualizations via our new filter approach. Several "columns" are visible as well, indicating turbulent behavior in directions being orthogonal to the equator and tangential to the Earth's surface

Abstract

This paper introduces a new and effective approach for visualizing complex magnetic fields. The paper defines a local approach for measuring the degree of local directional change of magnetic field vectors and uses this measure to generate volume visualizations that emphasize areas with highest values of locally integrated directional change of a vector field. The presented method was motivated by the need for having more effective tools supporting interactive exploration of the intricate magnetic field behavior captured in extremely large simulated data of the Earth's magnetic field. Of particular interest is a better understanding of the causal relationship between the Earth's convection phenomena (geodynamo) and the induced magnetic field, with high turbulent behavior in the Earth's core. The introduced local filter-based approach for visualization leads to a significant reduction in the amount of scientifically relevant data to be focused on in a rendering, and it therefore accelerates the overall scientific exploratory process. The viability of the method is demonstrated by specific examples.

1 Introduction

The Earth's magnetic field is generated by the motion of liquid iron alloy, so-called geodynamo. Numerical simulations of the geodynamo, other planets, and solar dynamos, present an enormous computational and visualization challenges. In geodynamo simulations, we need to represent a vast length scale form thickness of the boundary layer (0.1m) to outer core geometry (1000km) and time scale from rotation of the Earth (1 day) to magnetic field reversals (10^5 years) of the convection and magnetic fields. Consequently, geodynamo simulations requires extremely high spatial resolution and long time integrations. For this purpose, geodynamo simulations have been performed on some of the world's fastest computers. The geodynamo represents a major visualization challenge, as the output consists of time-varying vector and scalar fields representing turbulent convection in the Earth's core and the coupled magnetic field generated by that flow. The number of fields to be studied, the resolution required, and the long-time series makes extraction of features very challenging. Moreover, the observation used to compare against simulations is the magnetic field at and above the Earths surface far from the outer core which is modeled in the simulations, and we can only observe large scale magnetic fields generated in the outer core.

The results from the simulations show that we have a highly turbulent magnetic field in the inside (outer core) which stabilizes going further away from the center. It is assumed that the field itself is mainly induced by two main drivers, namely the α- and ω- effect [2].

The simulation itself is run on a large grid, such that visualizing the whole vector field as in Fig. 2, is lacking detailed insights of the emergence of the magnetic field. Increasing the problem size further to unsteady data, filtering comes more and more into account. In our first draw we fetch these effects visually, deriving a filter that is applied on the magnetic field (Section 2, Angular Direction Changing Rate), resulting in a less complex scalar field which then can be visualized with common techniques. This reduced complexity then leads the way for further analysis and visualization tasks. Our results are showing, that we can use our filter for example to

*TU Kaiserslautern, Computer Graphics & HCI Group, Germany, email:ruediger@rhrk.uni-kl.de
†UC Davis, Dept. of Computer Science
‡UC Davis, Dept. of Earth and Planetary Sciences

generate a "negative" picture of the highly turbulent magnetic field, thus visualizing the areas of the vector field that are only barely affected by one of the above mentioned effects.

One of the main challenges from the application scientist we want to tackle with our method described here, is to have a fast, reliable and easily interpretable visual output. Such that it enables us to visually perceive the influence of changes in the simulations parameter settings.

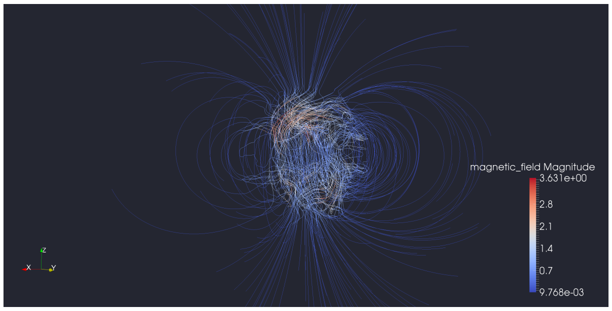

Figure 2: Streamline visualization using and extended domain, containing the simulation domain of the outer core and a potential field for the magnetic field outside the simulation domain. Using 100 seed points placed in sphere around the center for streamline tracing. Showing of the dipole structure of the magnetic field as also known from physical experiments.

1.1 Related Work

First attempts for visualizing geomagnetic data were made by Ohno et al. [7] and especially for the flow in the mantle by Schröder et al. [8]. A good overview on basic techniques of vector field visualization was provided by Salzbrunn et al. [10], Brambilla et al. [1] and Zhenmin-Peng et al. [9]. They showed and provided examples of the most common techniques covering feature-based and partition-based flow field visualization. We have combined a couple of these techniques in the visualization of our data of interest, using user-defined features and filters for a kind of partitioning of the data without doing a full blown topological analysis. Marchesin et al. [5] showed an interesting approach using streamlines in complex datasets. They precompute a random set of streamlines and select the shown streamlines depending on the actual view. When necessary their method seeds new lines in empty regions. Although it could help to identify regions of interest, we need to have more user control for the complex vector fields in our field of application. A different approach for dealing with crowded scenes was presented by Mehran et al. [6], which is also mainly tailored to flow visualization. Clearly, there exists a need for a more specific/adapted approach. Our approach extends the one from Daniels et al. [3], which also covers the problem of interactive feature processing, for the use in geophysics visualization and our special needs. Finally the visualization system we used is based on the system introduced by Kreylos et al. [4].

2 Method Description

To reduce the overall complexity we first want to depict the macroscopic behavior. But our simulation domain is limited to the core and mantle. To visualize whats happening outside the domain we can use a precomputed potential field as used in Fig. 2, leading to an exponentially increasing size of the data set (We have $4*10^6$ vertices to describe only the outer core with an respective diameter of 3,471 km compared to 6,371 km to only fetch the magnetic field near the Earth's surface, we would need an additional 2.5 times of vertices or 10 times the number of voxels). To avoid this massive scaling we are using the spherical harmonics analysis to determine

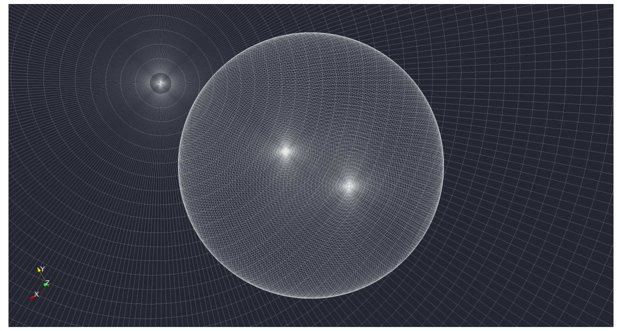

Figure 3: Depiction of the cell structure of the underlying data. An unstructured grid is used for the description. The size of the cells vary with increasing radius. As well when going from top to bottom. In itself the structure is regular, which means the size changes linear with the components (in spherical coordinates) and finer in radial direction near the boundaries. The dataset covers only a shell of a sphere, because the inner core is excluded from the simulation.

the value of the magnetic field at any given location beyond the Earth's surface (see Equations 1 and 2). Whereas a single evaluation of a point can be done quite efficiently, the evaluation of multiple ones as needed for streamline visualization is getting inefficient. Thus we are interested in drawing the minimum number of streamlines to depict the overall structure. Therefor we are deriving a filter that fetches areas of same behavior. Due to the fact that magnetic field lines cannot penetrate each other, the separation can be reduced to finding only the boundaries of these areas, as seeding streamlines in between would reveal the same behavior.

$$\mathbf{B} = -\nabla W, \tag{1}$$

where W is the magnetic potential. W is described by a series of Gauss coefficients g_l^m and h_l^m by

$$\mathbf{B} = \sum_{l=1}^{l} \sum_{m=0}^{l} R_e \left(\frac{R_e}{r}\right)^{l+1} \left[g_l^m cos(m\phi) + h_l^m sin(m\phi)\right] P_l^m(\theta), \tag{2}$$

where R_e is the respective earth radius and P_l^m are the normalized Legendre polynomials. ϕ, θ and r are the spherical coordinates.

2.1 Filter Definition: Angular Direction Changing Rate

The main idea behind this filter applied onto the magnetic field, is to catch the effect of the main drivers, such it can be used to visualize only those magnetic field lines that are inducing the main behavior. As we do not know directly how the α- and ω- effect is defined, we focus on fetching the areas that are most probably effected by these or visa versa. This can be achieved by finding those areas, that vary significantly from the rest. In our case we depict the variation as the difference in the directions of the vector field for a specific range around each vertex in the dataset. We used a k-nearest-neighbor (kNN) approach for the range to avoid errors that could arise through the chosen interpolation method. Our feature is defined as:

$$ADCR(v) = \sum w_i * acos\left(\frac{< v, n_i >}{||v||||n_i||}\right) \tag{3}$$

where v is the current vertex we want to determine the variation for, the n_i depict the k nearest neighbors, $<', '>$ denotes the scalar product and $||*||$ the Euclidean norm for vectors. The differences of the k nearest neighbors are weighted with respect to their distances using least squares.

$$w_i = \frac{dist(v,n_i)}{\sum_{j=0}^{k} dist(v,n_j)} \text{ , with} \quad (4)$$

$$dist(v,n_i) = ||(n_i - v)|| \quad (5)$$

As we want to filter out those regions that are significantly different from the others, we modeled this significance with the following function:

$$f(ADCR) = e^{\lambda(ADCR-\pi)} \quad (6)$$

Following this approach, we have a smooth function which emphasizes high changes and discriminate the lower ones. Thus the resulting value increases the more the angular differences reaches the maximum of π and additionally norms the value range to $[0,1]$, which makes it easier for visualization and interpretation. We can now choose λ, such that we fetch only the desired changing rates and separate the regions of interest, see Fig. 4 to determine the λ value.

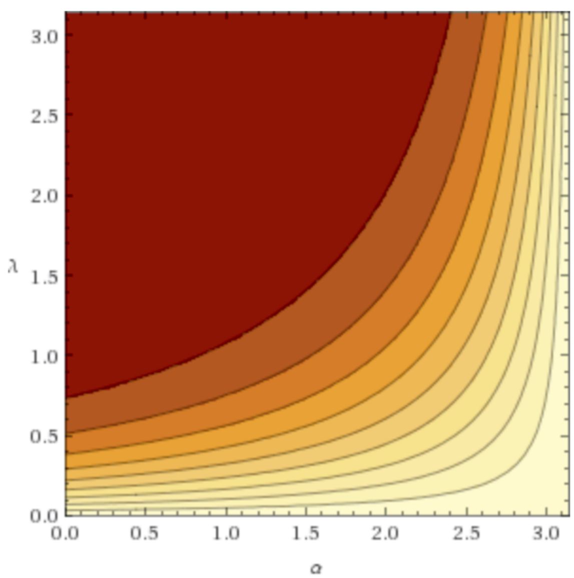

Figure 4: Effect of the significance function on the resulting ADCR value. α represents the calculated angle difference. λ is chosen according to the desired angle threshold. It is modified until the desired effect can be visually distinct.

2.1.1 Efficiency

We briefly discuss the complexity of the proposed filter. The data itself is a subset of the original one, with only 10^7 vertices, compared to 10^{10}. The dataset is arranged as an unstructured grid covering a shell of a sphere, namely the Earth's liquid outer core (see Fig. 3). Looking at the mathematical definition there are two main drivers for our complexity examination, the number of vertices in the selected subset, now denoted as n and the number of neighbors taken into account k. The computation itself is parted in five steps. First we need to get the k nearest neighbors. Second we compute the *acos*. Third we compute the weights for each neighbor difference, which mainly is a distance computation. Fourth we need to sum up the results. Lastly we need to do this for all vertices in the subset. For step (1) we precomputed a kd-tree, so that we can take an average complexity of $O(logN)$. We assume that the kd-tree is computed for the whole dataset with N vertices, because in most cases we will use it for more then one subset, amortizing the initial costs. Regarding the large number of vertices we have in total, we need to keep in mind, that the kd-tree itself will also need a significant amount of memory capacity. Step (2) and (3) are computed k times per vertex. Assuming (2) and (3), (4) can be done efficiently we get an average complexity for Step (5) of $O(k*n)$. Our experiments have shown that choosing k in the range of $[5,10]$ is sufficiently enough to get valuable results. Thus the complexity of Step (5) can be simplified to $O(n)$. The overall complexity for the computation of the ADCR is therefore $O(logN) + O(n)$. Step (5) can be parallelized easily (splitting up the computation for multiple smaller subsets of vertices) reducing the computation time significantly.

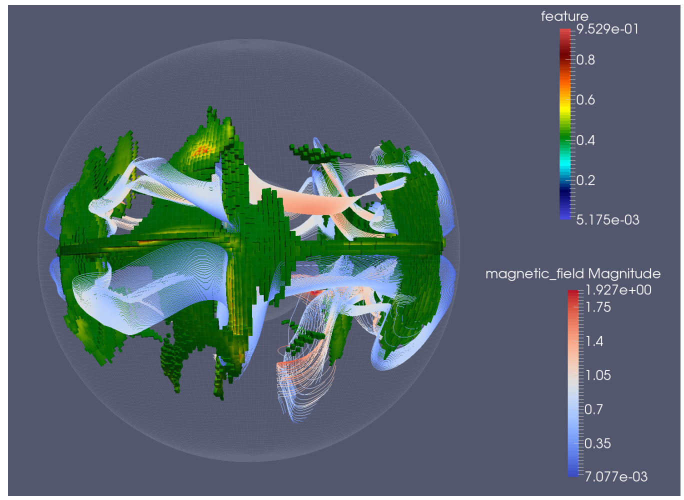

Figure 5: Full sized visualization of the magnetic field using ADCR for seeding in all topological relevant areas including ADCR visualization using threshold volume. View from equator.

3 Results

The most valuable result for the geophysics is shown in Fig. 5 and Fig. 6d, turbulent areas are highlighted by the ADCR and can be found in the equatorial plane and the area where he magnetic field lines go to higher latitude. There are two important process in the dynamo, namely the ω-effect and α-effect. The ω-effect is the extension of the magnetic field lines by the differential rotation. The α-effect is the process in which magnetic field lines are twisted by the helical flow (such as the convection columns). With typical methods for seeding and visualization it was very hard to depict those effects. Fig. 6 provides a good comparison. First we tried simple approaches for seeding streamlines. With exploratory seeding based on a point location, the limits of a structural perception reached their limits very fast. With a high resolution line source we made some first progress in fetching interesting behaviors (see Fig. 6a and Fig. 6b). As already known by the geophysics the effects seem to appear in the equatorial regions and normal to it (rotation axis). Using these insights, it was still hard to perceive structural patterns in the magnetic field. The next approach was to use the areas where vorticity's z-component is vanishing (see Fig. 6c). This revealed some first patterns, as one can see that the field lines are arranging nearly parallel and seem to have no significant turbulence in this areas. We then introduced the ADCR to depict areas of high turbulence to compare them against areas with low turbulence. Using these two counterparts as input for our seeding strategy we come up with a visualization that reveals a structural pattern, that was not visible before. Fig. 6d and Fig. 5 shows how our method helped to gain insight in a structural pattern that is correlated by the geophysics with the α-effect.

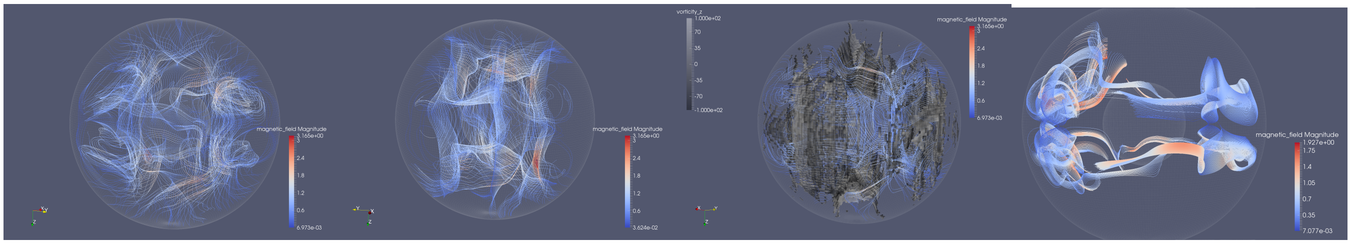

(a) Equatorial axis parallel (b) Rotation axis parallel (c) Vanishing vorticity z-component (d) ADCR

Figure 6: Comparing different strategies for seeding streamlines to visualize the magnetic field. All seeding is done by a high resolution line source. Fig. 6a and Fig. 6b using regularly spaced lines parallel to the respective axis in the middle of the domain. Fig. 6c generated by placing the lines inside the vanishing z-component areas. Fig. 6d seeding in high turbulent areas and in encapsulated low turbulent areas (wholes in Fig. 5).

Regarding the large amount of unstructured data we were working with, our system approach tackles this problem efficiently. We provide an approach that is highly concurrent. At first we are using our filter the angular direction changing rate from Section 2.1 to explore regions of interest. Afterwards we are using a volume threshold to depict high turbulent areas and to analyze the impact in all three dimensions. We completed the visualization of turbulence with a multilayer isosurface. To further study the correlation of the ADCR with the overall magnetic field we exploit the structure of the volume threshold visualization to seed streamlines for the magnetic field and thus get an impressive output of the field's behavior with reduced complexity for further analysis tasks. As the proposed method for the ADCR is highly concurrent, we are able to reduce the time for analysis for the geophysics dramatically.

3.1 Application Scientists Insights

In the present visualization, intense ADCR mainly locates lower latitude near the CMB. And, the magnetic field lines starting from this area stay in the low latitude without going out from the higher latitude. We consider that the the magnetic field in the turbulent flow in the lower latitude is extended in the longitudinal direction by the ω-effect in the area where ADCR is weak, and twisted towards the higher latitude by the α-effect at the convection column with larger ADCR. We expect that the large ADCR in the mid-latitude represents the area where the magnetic field is twisted by the α-effect because the dipolar magnetic field (or intense z-component) is generated by the α-effect. In Fig. 2 one can see, that the equatorial plane induces a structural separation of the magnetic field, which shows that the magnetic field line crossing the equatorial plane is twisted to the zonal direction by the differential rotation. In this study, we treat the magnetic field by ADCR, but this method is applicable for the arbitrary vector field. We expect that we can extract effects of the turbulence by specifying the length scale to investigate effects of the magnetic field generation by turbulent flow in the Earth's outer core. We also expected if we can extract what length scale flow and magnetic field contribute the generation of dipole component of the magnetic field.

Further we are now able to visually perceive changes in the simulations parameter settings, which were very hard to track before due to the complex behavior of the vector field. Additionally we could now study the effect of these parameters separately for the α-effect. We look forward to find a similar method for the other effects as well.

4 Conclusions

We have introduced a filter that effectively reduced the complexity for visualizing the Earth's magnetic field. We have shown that our approaches allow a scientist to rapidly explore a highly complex simulated magnetic field data set, making it possible to quickly recognize regions in the field characterized by interesting and possibly not yet fully comprehended behavior. Our filter should be a viable tool for geophysicists for a variety of relevant purposes, including a deeper understanding concerning the influence of a simulations input parameters, the formulation of new scientific hypotheses, and the identification of potential flaws in a specific implementation of a simulation method.

We have shown that the proper use of well established visualization techniques already provide a good first visualization, but we have also shown that it lacks of appropriate filters especially for visualization. Typical flow field approaches do not satisfy this need and for more advanced magnetic field visualizations, which leads to the need of new approaches for visualizing 3D vector fields without motion.

5 Future Work

We only used a reduced part of the whole simulation here, but we also want to support the large data sets by the massively parallel simulation which is 1000 times larger than the present study. Additionally we want to support the extraction of a specific length scale of fields in this approach by choosing the range of neighbors taken into account, such that we can dynamically reduce the complexity of the data set during visualization. Currently the seeding is done manually regarding visual detected patterns. We look forward to automate this seeding procedure and this way to find a possibility to describe them analytically reducing the overall effort for computation. We did not cover time series yet, but looking at the emergence of detected patterns overtime as temporally evolving behavior is of major interest for the geophysics in the near future.

Acknowledgments

This work was supported in part by National Science Foundation awards EAR-0949446 and IIA-1125422.

References

[1] A. Brambilla, R. Carnecky, R. Peikert, I. Viola, and H. Hauser. Illustrative flow visualization: State of the art, trends and challenges, 2012.

[2] B. A. Buffett. Earth's core and the geodynamo. *Science*, 288(5473):2007–2012, 2000.

[3] J. Daniels, E. W. Anderson, L. G. Nonato, and C. T. Silva. Interactive vector field feature identification. *IEEE transactions on visualization and computer graphics*, 16(6):1560–1568, 2010.

[4] O. Kreylos, E. W. Bethel, T. J. Ligocki, and B. Hamann. Virtual-reality based interactive exploration of multiresolution data. In G. Farin, H.-C. Hege, D. Hoffman, C. R. Johnson, K. Polthier, B. Hamann, and H. Hagen, editors, *Hierarchical and Geometrical Methods in Scientific Visualization*, Mathematics and Visualization, pages 205–224. Springer Berlin Heidelberg, Berlin, Heidelberg, 2003.

[5] S. Marchesin, C.-K. Chen, C. Ho, and K.-L. Ma. View-dependent streamlines for 3d vector fields. *IEEE transactions on visualization and computer graphics*, 16(6):1578–1586, 2010.

[6] R. Mehran, B. E. Moore, and M. Shah. A streakline representation of flow in crowded scenes. In D. Hutchison, T. Kanade, J. Kittler, J. M. Kleinberg, F. Mattern, J. C. Mitchell, M. Naor, O. Nierstrasz, C. Pandu Rangan, B. Steffen, M. Sudan, D. Terzopoulos, D. Tygar, M. Y. Vardi, G. Weikum, K. Daniilidis, P. Maragos, and N. Paragios, editors, *Computer Vision – ECCV 2010*, volume 6313 of *Lecture Notes in Computer Science*, pages 439–452. Springer Berlin Heidelberg, Berlin, Heidelberg, 2010.

[7] N. Ohno and A. Kageyama. Scientific visualization of geophysical simulation data by the cave vr system with volume rendering. *Physics of the Earth and Planetary Interiors*, 163(1-4):305–311, 2007.

[8] S. Schröder, J. Peterson, H. Obermaier, L. H. Kellogg, K. Joy, H. Hagen, et al. Visualization of flow behavior in earth mantle convection. *Visualization and Computer Graphics, IEEE Transactions on*, 18(12):2198–2207, 2012.

[9] Z. P. S.;Laramee. Higher dimensional vector field visualization: A survey. *EG UK Theory and Practice of Computer Graphics*, 2009.

[10] Tobias Salzbrunn, Heike Jnicke, Thomas Wischgoll, and Gerik Scheuermann. The state of the art in flow visualization: Partition-based techniques. *SimVis*, 2008.